

## Full Length Article

# The novel approach to physico-chemical modification and cytocompatibility enhancement of fibrous polycaprolactone (PCL) scaffolds using soft X-ray/extreme ultraviolet (SXR/EUV) radiation and low-temperature, SXR/EUV induced, nitrogen and oxygen plasmas

Joanna Czwartos<sup>a,\*</sup>, Angelika Zaszczynska<sup>b</sup>, Agata Nowak-Stepniowska<sup>a</sup>, Tomasz Fok<sup>a</sup>, Bogusław Budner<sup>a</sup>, Andrzej Bartnik<sup>a</sup>, Przemysław Wachulak<sup>a</sup>, Dorota Kołbuk<sup>b</sup>, Paweł Sajkiewicz<sup>b</sup>, Henryk Fiedorowicz<sup>a</sup>

<sup>a</sup> Institute of Optoelectronics, Military University of Technology, 2 Kaliskiego St., 00-908 Warsaw, Poland

<sup>b</sup> Institute of Fundamental Technological Research, Polish Academy of Sciences, Pawińskiego 5B, 02-106 Warsaw, Poland

## ARTICLE INFO

## Keywords:

Soft X-ray/extreme ultraviolet (SXR/EUV) radiation  
Low-temperature plasma treatment  
Electrospun polycaprolactone (PCL) nonwovens  
XPS analysis  
L929 mouse fibroblasts  
Cytocompatibility enhancement

## ABSTRACT

The fundamental aspect of the fabrication of microporous, fibrous biomaterials in form of scaffolds is the optimization of their surface properties to enhance cellular response. In this work, a novel approach to physico-chemical modification and bioactivity enhancement of electrospun fibrous polycaprolactone (PCL) nonwovens using soft X-ray/extreme ultraviolet (SXR/EUV) irradiation and exposure to a low-temperature, SXR/EUV induced, nitrogen and oxygen plasmas is presented for the first time.

Chemical alterations and morphology of the fibrous structure of irradiated PCL mats were examined using X-ray photoelectron spectroscopy (XPS) and scanning electron microscopy (SEM), respectively. The impact of introduced changes on viability, morphology, and adhesion of L929 mouse fibroblasts was examined. It was found that simultaneous interaction of SXR/EUV radiation and N<sub>2</sub> or O<sub>2</sub> photoionized plasmas led to strong chemical decomposition of the surface of fibrous PCL mats. Also, mats' spatial porous structure was not damaged and the fibers were not broken or fused. All modified samples demonstrated cyto-compatible and non-cytotoxic properties. Enhancement of L929 cell adhesion and increased proliferation were also observed.

## 1. Introduction

Biomaterials in the form of microporous scaffolds, with a strongly developed three-dimensional spatial structure, are used in regenerative medicine as temporary substrates providing an appropriate environment for the regeneration of damaged tissues and organs. These substrates are generally designed to serve as the temporal extracellular matrix (ECM), allowing the differentiation and proliferation of the deposited cells [1–3]. The success of the treatment process highly depends on the properties of such three-dimensional biomaterials. In order to accelerate the regeneration and obtain new, fully functional tissue, it is necessary to adjust the physicochemical and mechanical properties of the scaffold to the parameters of the tissue being replaced [4–6]. The degradation time of a biomaterial is also of high importance. It should be well synchronized with the time of the regeneration process to ensure optimal conditions

throughout the healing period [7,8]. For this reason, biodegradable and biocompatible polymers such as aliphatic polyesters including polyglycolide (PGA), polylactide (PLA), or polycaprolactone (PCL), and their copolymers, are widely used to construct scaffolds used for regenerative medicine. Specifically, PCL has attracted the attention of many researchers. This material is a semi-crystalline aliphatic polyester, exhibiting good chemical stability, high mechanical strength, and unique viscoelastic properties. However, due to its relatively low hydrophilicity and lack of active functional groups on its surface promoting the adsorption of proteins, the affinity of cells to this hydrophobic polymer is limited. Therefore, it is very important to modify it appropriately to overcome these disadvantages and significantly improve its bioactivity to increase the potential of using this material in tissue engineering.

Many techniques have been used for PCL scaffolds modification, including laser treatment [9], grafting or coating with gelatin or other

\* Corresponding author.

E-mail address: [joanna.czwartos@wat.edu.pl](mailto:joanna.czwartos@wat.edu.pl) (J. Czwartos).

<https://doi.org/10.1016/j.apsusc.2022.154779>

Received 1 July 2022; Received in revised form 31 August 2022; Accepted 1 September 2022

Available online 6 September 2022

0169-4332/© 2022 The Authors. Published by Elsevier B.V. This is an open access article under the CC BY-NC-ND license (<http://creativecommons.org/licenses/by-nc-nd/4.0/>).

natural polymers [10–13], composing or coating with micro- or nanoparticles (carbon nanotubes (CNTs), hydroxyapatite (HA), bioglasses (BGs)) [7,14,15], chemical modifications [16,17] and the most popular and universal technique of scaffold bioactivation: low-temperature plasma treatment [18–21]. Exposure of scaffolds to cold plasma leads to several changes on their surface: crosslinking, surface ablation, nano- or micropatterning, strong chemical structure alterations such as atoms or polar functional groups incorporation (e.g.  $-\text{COOH}$ ,  $-\text{COO}$ ,  $-\text{NH}_2$ ,  $-\text{OH}$ , etc.). As a result, the hydrophobic character of scaffolds changes to hydrophilic, and its cytocompatibility is enhanced. It is worth noting, however, that the plasma treatment effect on polymer surfaces, particularly the wettability properties observed, is not permanent and changes over time. It is related to the polymer aging process. Aging time is different for each polymer and strictly depends on the plasma parameters used and the chemical structure of a polymer. Wettability improved right after plasma exposure (i.e. decrease of surface contact angle), can deteriorate over time, and in some cases return to original values or values very close to original ones [22–26].

The effect of plasma treatment on the physicochemical properties of scaffolds and cell-scaffold interactions has been examined by many scientific groups. For example, Asadian et al. [21] observed that  $\text{N}_2$ , Ar, and the mixture of He/ $\text{NH}_3$  plasma treatment of PCL scaffolds induced strong chemical changes in their structure, i.e. grafting of a polar group, containing oxygen or nitrogen atoms, which significantly improved the wettability of scaffold fibers. On the other hand, such treatment did not noticeably affect the fiber structure of the scaffold. All three variants of plasma functionalization of PCL scaffolds had noticeable, positive effects on human foreskin fibroblast (HFF) cell adhesion and proliferation. The most explicit cell adhesion and proliferation effect were observed for the scaffold fibers treated with Ar plasma. Examinations conducted by Martins et al. [27] also showed that treating electrospun PCL nanofiber meshes with Ar (and  $\text{O}_2$ ) plasma led to strong adhesion and increased cell viability, in this case, human umbilical endothelial cells (HUVEC), compared to unmodified PCL fibers. Other studies exhibited that surface modification of PCL scaffolds using low-temperature plasma can positively impact their adhesion abilities which are very important in terms of adjusting the coating features to specific therapeutical needs [28–30].

The goal of the paper is to present a novel, alternative technique of modifying organic polymers, including the nanofibrous form of scaffolds, used in biomedicine and tissue engineering, which has never been presented before. This technique is based on the photoionization of gases (in this case nitrogen or oxygen), with nanosecond soft X-ray (SXR) and extreme ultraviolet (EUV) pulses, coming from laser-produced Xe plasma (LPP). Exposing polymers to SXR/EUV radiation leads to ablation, topography changes in their structure, and strong chemical decomposition [31–34]. Moreover, when low-temperature plasma induced by SXR/EUV irradiation in a gas (oxygen or nitrogen) is used at the same time, new functional groups appear and nitrogen or oxygen atoms are incorporated into the structure of modified polymers.

In our previous papers so far [35–38], polymers were modified using the experimental setup in which low-temperature plasma was induced through irradiation of a small portion of gas (e.g.  $\text{N}_2$ ,  $\text{O}_2$ ) with a focused EUV beam. An ellipsoidal collector was used for this, which effectively focused radiation emitted from laser-plasma. However, using this collector during irradiation and modification of polymer surfaces leads to its gradual degradation as various decomposition products from irradiated polymers deposit on its reflective surfaces. This, in turn, decreases its reflection coefficient in the EUV range. To avoid these disadvantages, the new arrangement of the experimental setup was used for the first time for the research described in this paper. In this case, no SXR/EUV collector was used and the laser beam was focused directly on the Xe/ $\text{O}_2$  or Xe/ $\text{N}_2$  double-stream gas puff target (stream of Xe gas coming from the nozzle is surrounded by nitrogen or oxygen). Interaction of laser beam with Xe results in the creation of high-temperature laser-plasma which emits radiation in SXR and EUV range. This radiation ionizes  $\text{O}_2$  or  $\text{N}_2$  gas surrounding the Xe stream and leads to the creation of low-

temperature  $\text{O}_2$  or  $\text{N}_2$  plasma. Irradiation parameters (i.e. laser pulse energy, number of pulses, a distance of SXR/EUV, and photoionized plasma source from the sample) were optimized and adjusted so that low-temperature  $\text{O}_2$  or  $\text{N}_2$ -based plasma is the dominant factor that affects the modification process. It was important to ensure that radiation coming from laser-plasma is low enough to have no destructive effect on the sheer structure of the sample, and specifically not to lead to the melting of nano- and microfibers of the scaffold.

The effect of SXR/EUV radiation and low-temperature plasma ( $\text{N}_2$  or  $\text{O}_2$ ), achieved using the new arrangement of the experimental setup, on the chemical composition and morphology of PCL scaffold surfaces was examined using X-ray photoelectron spectroscopy (XPS) and scanning electron microscopy (SEM), respectively. Also, the impact of physicochemical changes of modified PCL samples on the viability, morphology, and adhesion of L929 mouse fibroblasts was evaluated.

## 2. Materials and methods

### 2.1. Fabrication of electrospun PCL nonwovens

The polycaprolactone (PCL) fibrous nonwovens were fabricated using the electrospinning machine (FLUIDNATEK® LE-5, Bioinicia, Spain) with Air Conditioning (Bioinicia, Spain) at room temperature and humidity of ~40 %. PCL (Mw = 80.000 g/mol, Sigma-Aldrich, UK) was dissolved in a solvent mixture of acetic acid: formic acid (1:9) (Sigma-Aldrich, UK), at a concentration of 12 wt% according to our protocol [39]. A high-voltage power supply (12 kV) was applied to the needle of the electrospinning apparatus, while the needle tip-to-collector distance was fixed at 100 mm and the flow rate of the polymer solution was 600 ml/h. The PCL mat was deposited on the aluminum foil (thickness of 30  $\mu\text{m}$ , Rotilabo®, Roth Selection, Germany), which was attached to the collector. The thickness of the mat obtained was 600  $\mu\text{m} \pm 18 \mu\text{m}$ . After the electrospinning process, all mats were placed under the fume hood to evaporate solvents in the fibers.

### 2.2. Modification of PCL nonwovens

A laser-produced plasma (LPP) soft X-ray/extreme ultraviolet (SXR/EUV) source, driven by 10 Hz Nd:YAG, was used for the modification of electrospun PCL nonwovens. The SXR/EUV source was based on a double-stream gas-puff target irradiated with an Nd:YAG laser (NL 129, EXPLA) producing 8 ns in duration, 2.1 J energy pulses. The gaseous target was created by the pulsed injection of a Xe gas into a hollow stream of nitrogen or oxygen (Xe/ $\text{N}_2$  or Xe/ $\text{O}_2$  target) using an electromagnetic valve system equipped with a double nozzle setup, synchronized with the laser system – Fig. 1. Interaction of a focused laser beam with the target results in the formation of a high-temperature Xe plasma emitting intense radiation in the SXR and EUV range which ionizes surrounding nitrogen or oxygen gas. As a result, the Xe laser-plasma is surrounded by low-temperature  $\text{N}_2$ - or  $\text{O}_2$ -based plasmas, induced by intense SXR/EUV radiation pulses.

Fig. 2 presents three SXR/EUV spectra from the gas puff target source. The first one is the emission spectrum from plasma created in the gas-puff target scheme in which the Xe is surrounded by He as a buffer gas. It is a basic variant of the SXR/EUV source based on a gas-puff target, described in our many previous publications [40,41]. The other two spectra are related to our current configuration, presented in this paper, in which the buffer gas He was replaced with  $\text{N}_2$  or  $\text{O}_2$ . In such cases, the intensity of SXR/EUV radiation decreases due to the absorption of radiation in  $\text{N}_2$  and  $\text{O}_2$ . This leads to the creation of low-temperature  $\text{N}_2$ - or  $\text{O}_2$ -based plasmas which can be used for surface processing, and at the same time, the remaining radiation interacts with the surface.

PCL polymer sample was exposed to one of these plasmas and to the part of the SXR/EUV radiation which was not absorbed by the gases. The exposure was performed using 10 SXR/EUV pulses. The polymer to be exposed was mounted on a tripod at a distance of ~11 mm from the

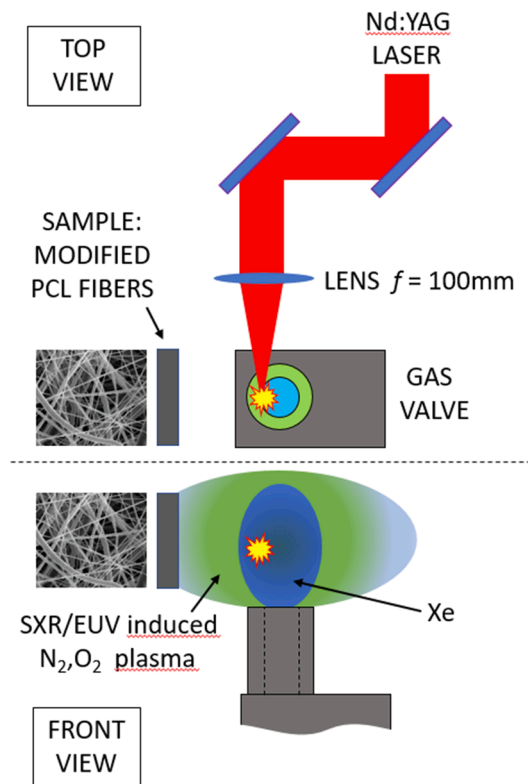


Fig. 1. Scheme of experimental arrangement for the modification of the fibrous PCL scaffolds with SXR/EUV radiation and low-temperature nitrogen and oxygen plasma.

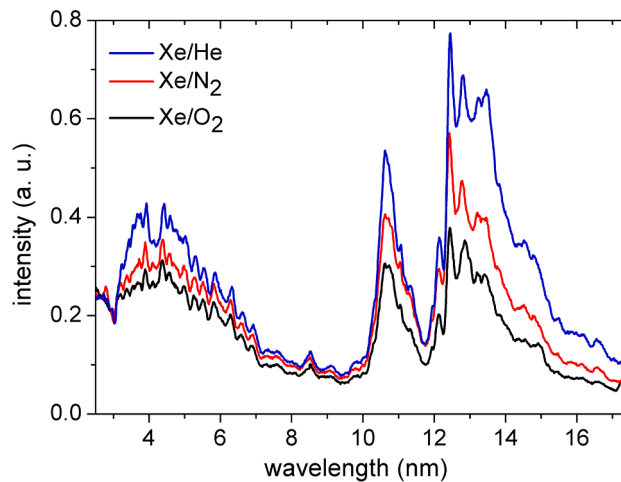


Fig. 2. The spectrum of the soft X-ray/extreme ultraviolet (SXR/EUV) radiation emitted from Xe plasma: created in a double stream gas-puff target scheme, with three buffer gases: He, N<sub>2</sub>, and O<sub>2</sub>.

nozzle setup. This resulted in a circular modification of the PCL area having a diameter of 5 mm. The setup presented and its novel configuration had never been used before for modification of the samples.

### 2.3. Characterization of PCL samples

#### 2.3.1. Morphology (SEM)

The morphology of non-modified and modified PCL nonwovens was analysed using scanning electron microscope SEM (JEOL JSM-6390LV, Japan). All samples studied were first coated with a gold layer of 5 nm thickness using a sputter coater (Smart Coater DII-29030SCTR,

Japan). During the scanning process, the acceleration voltage was 5 kV and the working distance was 5 mm. The SEM images of the PCL microstructures were used in order to measure the diameters of the fibers (100 measurements) with ImageJ software (v. 1.51j8, USA).

Total average porosity  $p$  was estimated as in our previous study [42] from the equation:

$$p = \frac{V_t - V_f}{V_t} = \left(1 - V_f \frac{\rho}{m_t}\right) = \left(1 - \frac{m_f}{m_t}\right)$$

where  $m_t$  is the hypothetical mass of solid sample determined as a product of volume occupied by a patch  $V_t$  and PCL density  $\rho$  (1.21 g/

$\text{cm}^3$ ), and  $V_f$  and  $m_f$  are real sample volume and mass, respectively. Average pore size  $P$  was estimated using the following equation [43]:

$$P = \frac{2D}{(1-p)}$$

where  $D$  is mean fiber diameter and  $(1-p)$  is average total projected area of fibers per unit area with  $p$  taken approximately as total porosity.

### 2.3.2. Chemical analysis (XPS)

Chemical analysis of untreated and modified PCL electrospun non-wovens with 10 SXR/EUV pulses and low-temperature  $\text{O}_2$  or  $\text{N}_2$  plasma was performed using X-ray photoelectron spectroscopy. XPS spectrometer (Prevac, Poland), equipped with SCIENTA R3000 analyser (VG Scienta, Sweden) and an X-ray lamp with Al  $K\alpha$  anode (Prevac, Poland), was used. During the measurements, the pressure in the ultra-high vacuum analysis chamber of the XPS system was about  $3 \times 10^{-9}$  mbar. High-resolution spectra in the narrow ranges of binding energy with a 40 meV step and pass energy of 100 meV for each band: C1s (281 eV–292 eV), N1s (395 eV–405 eV), and O1s (528 eV–538 eV) were recorded. The peaks related to C1s, N1s, and O1s bands were fitted using CasaXPS software. The background of Shirley type and Gaussian–Lorentzian (G–L) line shape (GL 50 for C1s, GL 60 for N1s, and GL 55 for O1s) were fitted for all these bands. All XPS spectra collected were shifted in such a way that the maximum of the C–C peak was at 285 eV.

## 2.4. Biological studies

### 2.4.1. Cell culture

L929 mouse fibroblasts (Sigma-Aldrich, Germany) were cultured in Dulbecco's modified eagle medium (DMEM, Sigma-Aldrich, Germany) supplemented with 10 % of fetal bovine serum (FBS, Thermo Fisher Scientific, Waltham, MA, USA) and 1 % of antibiotics solution containing 10 000 U/mL penicillin and streptomycin (Thermo Fisher Scientific, Waltham, MA, USA) following the manufacturer's instructions. The completed medium was replaced twice a week. Cells were subcultured via washing with phosphate-buffered saline (PBS, Life Technologies, USA) and trypsinized (trypsin-EDTA, Life Technologies, USA). Cells were maintained at 37 °C in a humidified atmosphere containing 5 %  $\text{CO}_2$ .

### 2.4.2. Presto Blue cell viability assay

The quantitative correlation between the Presto Blue (Thermo Fisher Scientific, USA) fluorescence signal and the cell number was done (data not shown). L929 fibroblasts were seeded on ethanol (Sigma-Aldrich, Germany) sterilized PCL samples placed in a 48-well plate in the amount of  $2.5 \times 10^3$  cells per well. Cells were grown in the incubator at 37 °C in a humidified atmosphere containing 5 %  $\text{CO}_2$  for 3, 5, and 7 days. Presto Blue reagent was added to cells for 2 h and fluorescence intensity was measured using the microplate reader system FLUOstar OPTIMA (Thermo Fisher Scientific, Waltham, MA, USA). The experiments were carried out with 6 replicates each.

### 2.4.3. Fluorescence microscope imaging of cellular morphology

L929 fibroblasts were cultured on PCL scaffolds placed in a 48-well plate in the amount of  $2.5 \times 10^3$  cells per well. After 1 and 3 days cells were rinsed in PBS (Life Technologies, USA) and were fixed with 3 % paraformaldehyde (PFA) (Sigma-Aldrich, Germany) for 30 min at room temperature. After permeabilization with Triton<sup>TM</sup> X-100 (0.1 % in PBS) (Sigma-Aldrich, Germany) for 5 min, F-actin was stained with ActinGreen<sup>TM</sup> 488 ReadyProbes<sup>TM</sup> (MolecularProbe, USA). The nuclei were counterstained with NuncBlue<sup>TM</sup> reagent (Invitrogen<sup>TM</sup>, USA). Stained cells seeded on the samples were visualized with a fluorescence microscope (Leica DMI3000B, Leica Microsystems, Wetzlar, Germany) using appropriate filters.

### 2.4.4. SEM imaging of cellular morphology

The cellular morphology of L929 cells cultured on PCL scaffolds was investigated using SEM. The PCL samples with fibroblasts were washed with PBS twice and fixed through immersion in glutaraldehyde (GA) (Sigma-Aldrich, Germany) for 1 h. Afterward, cells were cleaned with PBS (Life Technologies, USA) 3 times to remove toxic residuals of GA. Then, the specimens were dehydrated with ethanol solutions. The 30–100 wt% of ethanol (EtOH) Sigma-Aldrich, Germany) was applied in increasing order and exchanged every 30 min with EtOH/HMDS (hexamethyldisilazane) mixture (Sigma-Aldrich, Germany). Finally, samples were submerged in 100 % HMDS and left to dry under the hood. Samples were sputter-coated with 5 nm of a gold layer (Smart Coater DII-29030SCTR, Japan) and examined with the scanning electron microscope (JEOL JSM-6390LV, Japan) using a voltage of 10 kV.

### 2.4.5. Statistical analysis

Data were expressed as the mean  $\pm$  standard deviation (SD). The statistical analysis was performed in TIBCO Statistica 13.3 (TIBCO Software Inc, 2017, USA). To estimate the significant differences among viabilities of non-modified and modified PCL scaffolds, the factorial analysis of variance (Factorial ANOVA followed by Tukey's post-hoc test) was performed. Data were considered significant when  $p < 0.05$ .

## 3. Results and discussion

### 3.1. Morphological characterization of electrospun PCL nonwovens (SEM)

Scanning electron microscopy (SEM) images of pristine PCL sample and modified with SXR/EUV radiation and low-temperature oxygen and nitrogen plasma are presented in Fig. 3. As can be seen in subfigures, for all discussed cases, electrospun PCL nonwovens represent highly porous structures composed of randomly oriented, i.e. without any preferred orientation, interconnected nano-, and microfibers, with beadless morphology. For PCL pristine mat (Fig. 3a), it was found that the fiber diameter distribution is highly asymmetric with diameters ranging from  $\sim 150$  nm up to  $\sim 1250$  nm, an average diameter of  $718 \pm 26$  nm, and the dominant value of 850 nm. As can be seen in the SEM images, the structure of the PCL mats, when modified in the presence of low-temperature nitrogen or oxygen plasma, did not significantly change their porous, three-dimensional structure (Fig. 3b and 3c). Exposure to 10 several-nanosecond long SXR/EUV radiation pulses and photo-ionized plasmas did not lead to any damage to individual fibers and the overall structure of the mat. For two cases of modification, it was observed that the thinnest fibers in some parts of the mat structure (with the lowest diameters below  $\sim 400$  nm), were ablated due to photon induced fragmentation of polymer chains associated with a plasma thermal effect, leading to more symmetric fiber diameter distributions (Fig. 3b and 3c). As a result, the average values of the diameters of PCL scaffold fibers modified in plasma oxygen increased to  $792 \pm 18$  nm, while for PCL fibers, modified in the presence of nitrogen plasma this value was  $766 \pm 16$  nm. The corresponding dominant values were 850 and 750 nm, respectively. To sum up, the exposure of PCL samples to simultaneous radiation of laser-plasma and low-temperature oxygen and nitrogen plasmas did not significantly and, specifically, negatively affect the physical changes of the mat structure. The porosity of the analysed samples was  $\sim 76.2$  % and the mean pore size,  $P$ , was  $\sim 6$   $\mu\text{m}$ .

The examinations of the effect of low-temperature plasma modification of polymer scaffolds made of PCL on their morphology were also the subject of research by many other authors. They also observed a similar phenomenon of ablation of the thinnest fibers of the three-dimensional structure [18,27]. The disappearance of the thinnest fibers leads to the formation of empty spaces between the scaffold fibers, i.e. formation of micropores, which, as it turns out, may have a beneficial effect on cells. It has a positive effect specifically on some types of cells, such as fibroblasts, which can freely form an elongated cell body there

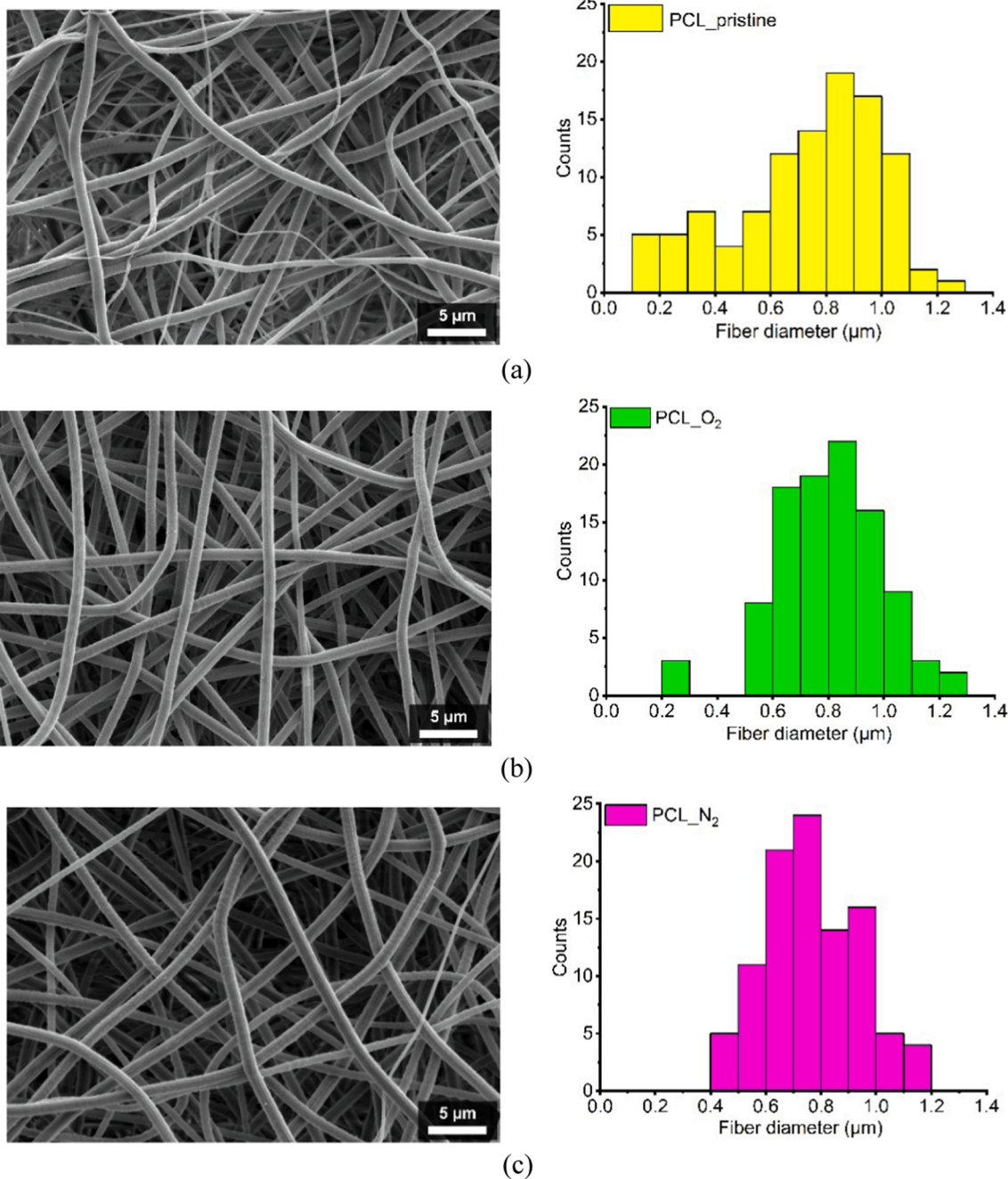


**Fig. 3.** SEM images of electrospun PCL nonwovens: (a) pristine and modified with SXR/EUV radiation and low-temperature (b) oxygen and (c) nitrogen plasma.

and spread out [44].

Other studies emphasize that the use of inappropriate parameters of the cold plasma treatment, such as too long exposure time may lead to the total destruction of the porous scaffold morphology which is a result of the fusing of the fibers. As a consequence, the scaffold becomes a structure that is unusable for tissue engineering applications [45].

### 3.2. Chemical analysis of non-modified and modified PCL electrospun nonwovens

The analysis of the chemical composition of unmodified and modified PCL electrospun nonwovens was carried out based on high-resolution XPS spectra. For this analysis, the model describing the C1s and O1s bands was used, developed based on non-modified reference PCL material in form of foil. The chemical structure of PCL mer is shown

in Fig. 4. Fig. 5a and 5b depict the XPS spectra: C1s and O1s band, respectively, for a non-modified reference PCL sample. Four peaks were modeled for this material's C1s band, representing the following chemical groups: C—C (carbon atom marked as C1) - at 285 eV (FWHM 1.3 eV), C\*—C=O(—O) (carbon atom marked as C2) - at 285.6 (FWHM

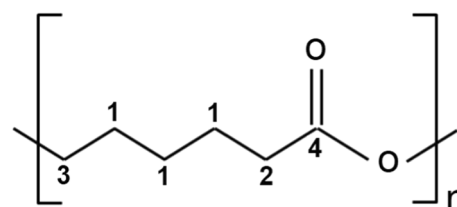


**Fig. 4.** Chemical structure of polycaprolactone's mer.

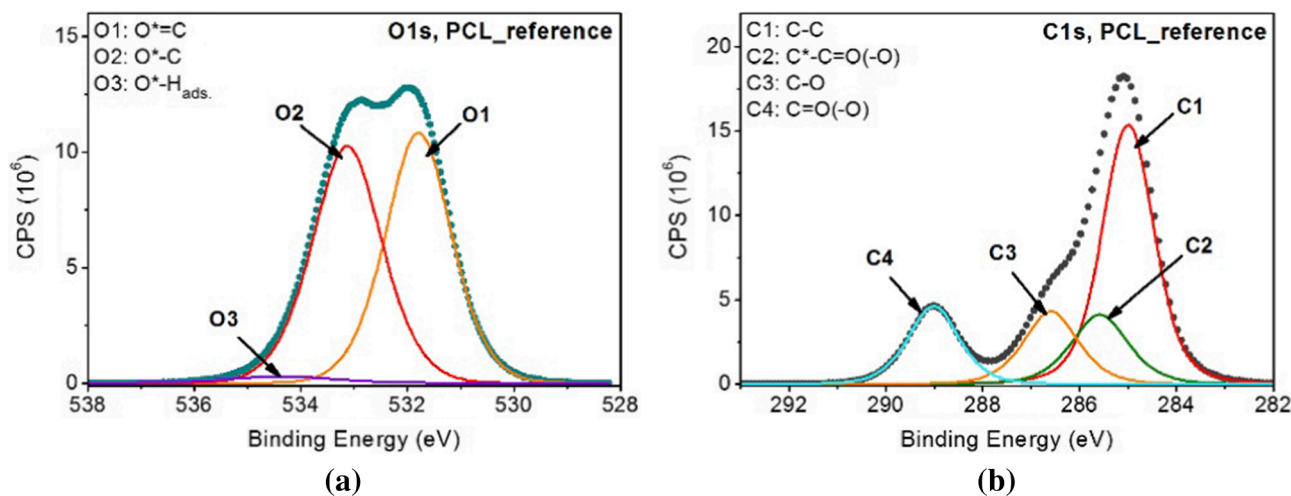


Fig. 5. XPS spectra of non-modified reference PCL material (in form of foil): (a) O1s band and (b) C1s band.

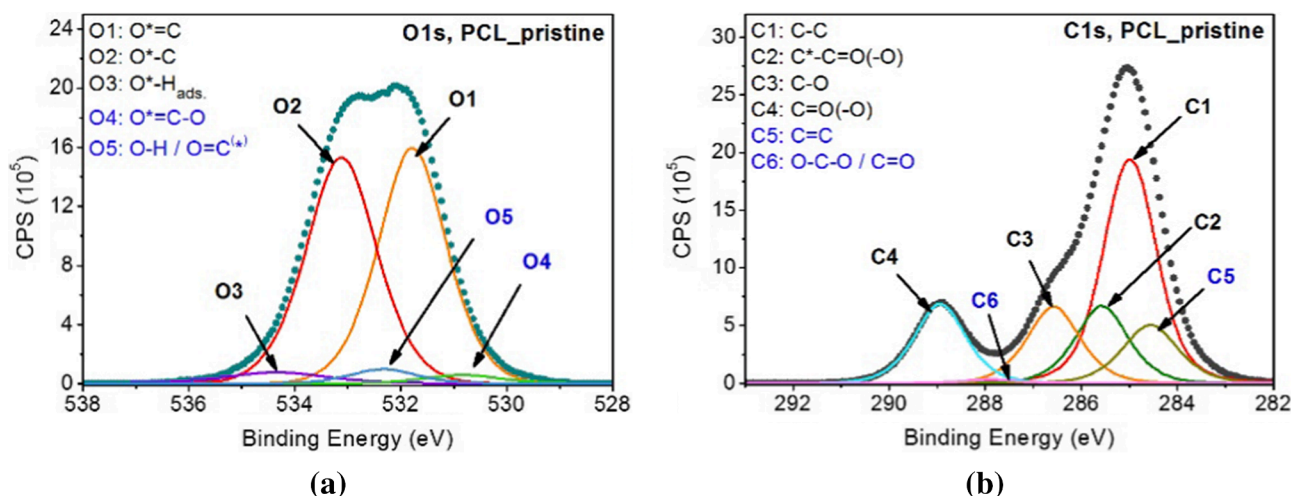


Fig. 6. XPS spectra of non-modified (pristine) electrospun PCL nonwoven: (a) O1s band and (b) C1s band.

Table 1

Binding energy range, FWHM range, and atomic concentration of different functional groups for reference PCL (in form of foil), PCL pristine, and PCL modified (reference PCL peaks given in rows are given in bold letters).

Symbol of the peak	Chemical group	Position (eV)	FWHM [eV]	PCL_reference (at.%)	PCL_pristine (at.%)	PCL <sub>N<sub>2</sub></sub> (at.%)	PCL <sub>O<sub>2</sub></sub> (at.%)
C1	C–C	285.0	1.3	40.31	32.68	23.36	20.75
C2	C <sup>+</sup> –C=O(O)	285.6	1.3–1.4	11.84	11.18	7.36	9.30
C3	C–O	286.6	1.3	11.84	11.18	7.36	9.30
C4	C=O(–O)	288.9–289.0	1.2–1.3	11.84	11.18	7.36	9.30
C5	C=C	284.6	1.4	–	8.91	20.73	19.63
C6	O–C–O/C=O	287.9	1.3	–	0.51	–	2.15
C7	CH <sub>3</sub> –C <sup>+</sup> –COO	285.9	1.3	–	–	0.73	1.56
C8	C–O–C	287.1	1.3	–	–	2.00	1.39
C9	C–N	286.1	1.3	–	–	4.00	–
C10	N–C=O/N–C–O	288.0	1.3	–	–	1.92	–
N1	N–C/N=C	398.9	2.1	–	–	4.00	–
N2	N–C=O	399.7	1.9	–	–	1.92	–
<b>O1</b>	<b>O=C</b>	<b>531.8</b>	<b>1.5</b>	<b>11.84</b>	<b>11.18</b>	<b>7.36</b>	<b>9.30</b>
<b>O2</b>	<b>O–C</b>	<b>533.1</b>	<b>1.5–1.6</b>	<b>11.84</b>	<b>11.18</b>	<b>7.36</b>	<b>9.30</b>
<b>O3</b>	<b>O–H<sub>ads.</sub></b>	<b>534.4</b>	<b>2.3</b>	<b>0.51</b>	<b>0.82</b>	<b>0.35</b>	<b>0.90</b>
O4	O=C–O/O=C–N <sup>(N2 modif.)</sup>	530.8–530.9	1.7	–	0.47	2.32	1.34
O5	O–H/O=C <sup>(*)</sup>	532.3	1.5–1.7	–	0.69	1.90	5.80

1.3–1.4 eV), C–O (carbon atom marked as C3) – at 286.6 eV (FWHM 1.3 eV), C=O(–O) (carbon atom marked as C4) – at 288.9–289.0 eV (FWHM 1.2–1.3 eV) and three peaks for O1s band, for the following

groups: O=C (oxygen atom marked O1) – at 531.8 eV (FWHM 1.5 eV), O–C (oxygen atom marked O2) – at 533.1 eV (FWHM 1.5–1.6 eV), O–H<sub>ads.</sub> (oxygen atom marked O3) – at 534.4 eV (FWHM 2.3 eV). The

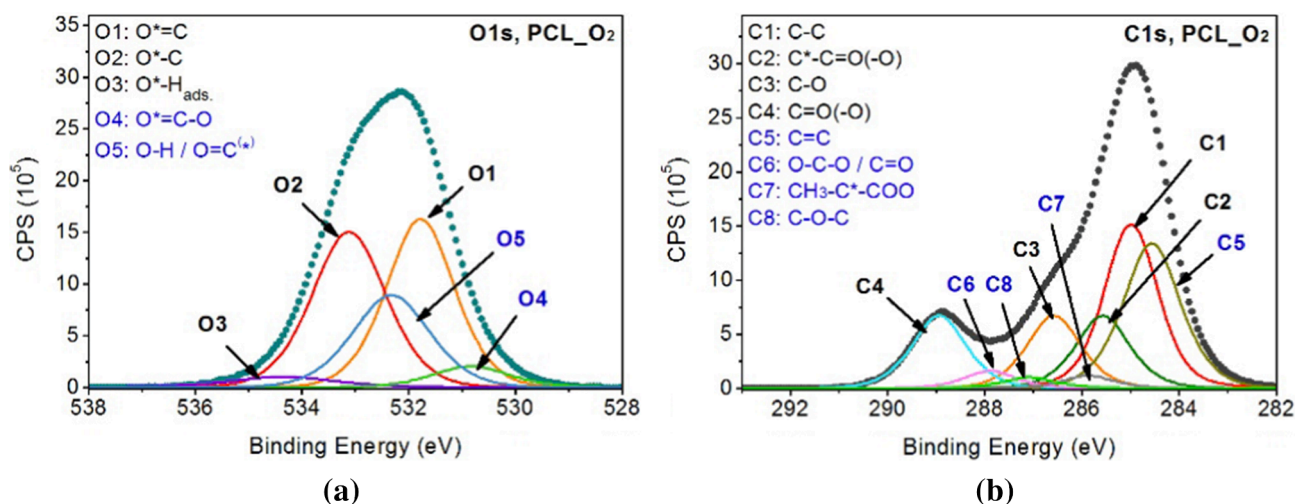


Fig. 7. XPS spectra of PCL nonwoven modified with SXR/EUV radiation and low-temperature oxygen plasma: (a) O1s band and (b) C1s band.

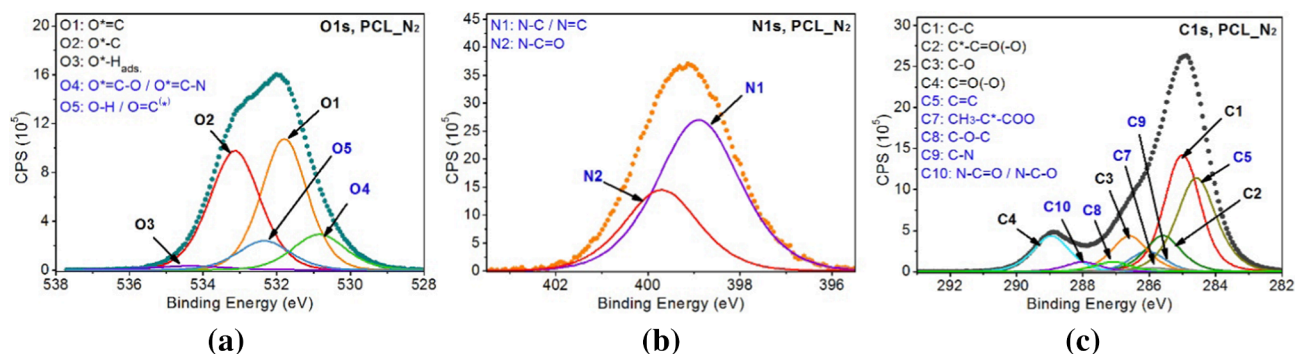


Fig. 8. XPS spectra of PCL nonwoven modified with SXR/EUV radiation and low-temperature nitrogen plasma: (a) O1s band, (b) N1s band, and (c) C1s band.

Table 2

The atomic concentration of carbon, nitrogen, and oxygen for reference PCL, PCL pristine, and PCL modified.

Elements	PCL_reference (at.%)	PCL_pristine (at.%)	PCL_N <sub>2</sub> (at.%)	PCL_O <sub>2</sub> (at.%)
C	75.8	75.6	74.8	73.4
N	–	–	5.9	–
O	24.2	24.3	19.3	26.6

model developed appropriately describes the chemical structure of PCL mer and is consistent with the literature [20,21].

The model developed for PCL foil was used for non-modified (pristine) PCL electrospun nonwoven. The XPS spectra for this sample are presented in Fig. 6. Two additional peaks were added to the bands C1s and O1s: C=C (C5) at 284.6 eV (FWHM 1.4 eV), O—C—O/C=O (C6) at 287.9 eV (FWHM 1.3 eV) and O=C—O (O4) at 530.8–530.9 eV (FWHM 1.7 eV), O—H/O=C<sup>(\*)</sup> (O5) at 532.3 eV (FWHM 1.5–1.7 eV), respectively, (it was assumed that O=C<sup>(\*)</sup> is formed when the structures O=C (O)O and O=C—O are formed). The presence of these additional functional groups in the non-modified nonwoven's C1s and O1s bands, compared to the reference PCL foil, can be the result of electrospinning being the process of fabrication, during which high voltage is applied. However, this can be confirmed through further research.

Next, the analysis of nonwovens modified with SXR/EUV radiation and low-temperature oxygen or nitrogen plasma was carried out based on the model developed for the pristine nonwoven. As demonstrated in previous papers, simultaneous irradiation of surfaces of various organic polymers with EUV radiation and low-temperature plasmas results in

their strong surface chemical decomposition [36–38,46]. EUV photon's energy is high enough to randomly break the atomic bonds in polymer chains and, as a result, form various functional groups and combinations of functional groups on their surfaces. On the other hand, the application of low-temperature plasma induced by EUV radiation near the polymer surface allows the introduction of additional atoms and functional groups which were not present in the original polymer material.

The results of the analysis of the modified PCL samples are presented in Table 1. For the PCL nonwoven modified with oxygen low-temperature plasma two additional peaks were introduced to the C1s band: CH<sub>3</sub>—C—COO (C7) at 285.9 eV (FWHM 1.3 eV) and C—O—C (C8) at 287.1 eV (FWHM 1.3 eV) – Fig. 7.

For the PCL nonwoven modified with low-temperature nitrogen plasma four additional peaks were introduced to the C1s band: CH<sub>3</sub>—C—COO (C7) – at 285.9 eV (FWHM 1.3 eV), C—O—C (C8) at 287.1 eV (FWHM 1.3 eV), C—N (C9) at 286.1 eV (FWHM 1.3 eV) and N—C=O/N—C—O (C10) at 288.0 eV (FWHM 1.3 eV) – Fig. 8. Since nitrogen atoms were incorporated into the surface of PCL fibers, an additional N1s band occurred. This band was modeled with two peaks representing the following functional groups: N—C/N=C (N1) at 398.9 (2.1 eV) and N—C=O (N2) at 399.7 eV (FWHM 1.9 eV), which correspond to the functional groups from C1s band with nitrogen in their structure, i.e. C9 and C10. The O1s band's peak, represented by the chemical group O=C—O for the pristine nonwoven and the one modified with oxygen plasma, in this case, due to similar binding energy, can be also represented by a chemical group in which a single-bonded carbon with oxygen is bonded with a nitrogen atom. Therefore, it can be represented by a group O=C—N.

Summing up, exposing PCL nonwoven to nitrogen plasma results in

the introduction of a significant amount of nitrogen into the nonwoven's structure. As Table 2 shows, the percentage content of nitrogen in the nonwoven modified with nitrogen plasma amounts to 5.9 at.%. When incorporated into the surface structure of PCL nonwoven fibers, nitrogen atoms displace oxygen atoms and the percentage content of the latter decreases to 19.3 at.%. The percentage content of oxygen in PCL foil and pristine PCL nonwoven was 24.2 at.% and 24.3 at.%, respectively, and the rest was carbon. As expected, modification with oxygen plasma leads to the increase of the percentage content of oxygen to 26 at.%, which is higher than ~2.3 at.% compared to reference PCL foil and nonwoven.

### 3.3. Cell attachment and growth investigation of L929 fibroblasts on plasma-treated PCL nonwovens

The introduction of physico-chemical alterations on the surfaces of fibrous polymeric structures used in tissue engineering has a tremendous and positive impact on cell behaviour. These changes can significantly enhance the properties of the scaffold in terms of its biocompatibility and bioactivity [47]. In previous sections, it has been shown that the usage of the new, alternative technique of modification, strongly changes the chemical composition of the surface of the scaffold fibers and simultaneously does not destroy the spatial structure of the scaffold. In order to evaluate how the presented technique, i.e. SXR/EUV radiation and low-temperature, SXR/EUV induced, O<sub>2</sub> or N<sub>2</sub> plasmas, affect cytocompatibility of the modified PCL scaffolds, viability, morphology, and cell spreading studies on L929 mouse fibroblasts were performed.

The viability of the L929 fibroblast cells on unmodified and modified PCL nonwoven surfaces is shown in Fig. 9. Tests were carried out using Presto Blue assay on days 3, 5, and 7 after cell seeding on PCL samples. As can be seen in the figure, the dependence of the effect on the type of plasma used during the modification process was clearly noted. The viability of cells on the PCL fibers modified with oxygen and nitrogen plasma increased significantly after 3, 5, and 7 days compared to the results on the control sample (not exposed to plasma). Moreover, a significant increase in L929 viability between the 3rd and 7th day and the 5th and 7th day for both plasma-treated conditions was revealed. Finally, on the 7th day of cell culture, a significant increase in cell viability under oxygen plasma compared to nitrogen plasma and untreated PCL nonwoven was also noted. Obtained results revealed that all the tested PCL samples were not cytotoxic. However, a strong effect of oxygen plasma conditions on the viability of L929 fibroblasts compared to nitrogen plasma treated PCL and untreated sample was proven.

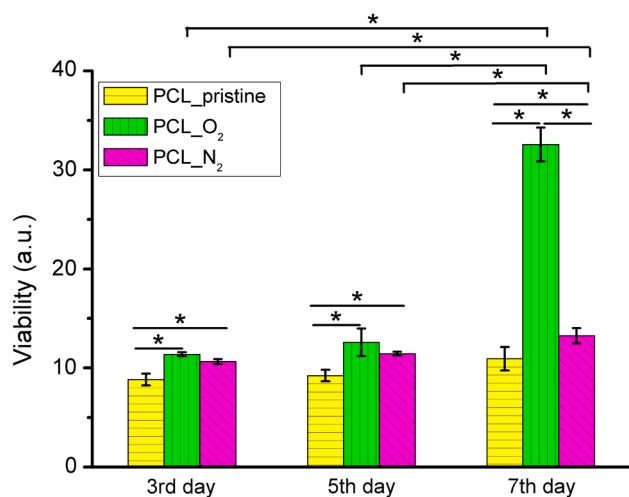


Fig. 9. Cell viability of L929 cells cultured on PCL samples non-modified and modified with SXR/EUV radiation and low-temperature oxygen and nitrogen plasma for 3, 5, and 7 days post-seeding. Error bars represent the standard deviation of the mean. Results were considered significant when  $p^* < 0.05$ .

The cellular spreading and proliferation of L929 fibroblast cells on unmodified and modified PCL nonwoven surfaces is presented in Fig. 10. For that reason, the cells were stained for F-actin and DNA and fluorescence was visualized with a laser scanning confocal microscope. Tests were carried out on 1 and 3 days after cell seeding on PCL samples. The 24-hour cultivation of cells on the tested surfaces did not show differences in the number of cells. However, cells grown on PCL scaffolds modified with oxygen and nitrogen plasma were better spread and elongated compared to round fibroblasts on unmodified PCL. After 3 days of L929 cell cultivation on the tested samples, a increase in proliferation of cells on both plasma-modified surfaces was revealed compared to the untreated PCL. As mentioned above, differences in the cell behaviour on PCL samples were indicated with yellow arrows in the figure. Moreover, the greater proliferation on the surface modified with oxygen plasma compared to the nitrogen plasma treated PCL was noted, thus the results are in agreement with data from the performed viability test. Furthermore, greater elongation and spread of fibroblasts providing better adhesion were observed on the oxygen plasma-modified surface. A similar effect was observed with SEM imaging presented in Fig. 11. Well-adhered cells with a flattened morphology and filopodia formation were observed on the 3rd day of the cultivation on the oxygen plasma-treated surface compared to untreated PCL and nitrogen plasma-treated surfaces.

The correlations between various types of plasma modification of PCL and increase in cell adhesion as well as proliferation and viability were shown in numerous publications. Recek et al. [48] investigated the influence of O<sub>2</sub>, NH<sub>3</sub> or SO<sub>2</sub> plasma treatments of PCL scaffold on HUVEC. The highest viability and adhesion of HUVEC on O<sub>2</sub> and NH<sub>3</sub> plasma-treated surfaces were revealed. Furthermore, O<sub>2</sub> and NH<sub>3</sub> plasma-treated samples showed enhanced endothelialization of this material. Siri et al. [19] observed an increase in adhesion of NIH 3 T3 murine fibroblasts due to the air plasma treatment of PCL. Modification made the surface more suitable for tissue engineering because of the increased surface hydrophilicity. Asadian et al. [21] observed higher viability of HFF cells due to N<sub>2</sub>, He/NH<sub>3</sub>, and Ar plasma modification of PCL nanofibers compared to the untreated sample with the strongest impact of Ar plasma treatment. Improved cell attachment and viability of 7F2 osteoblasts on PCL modified with O<sub>2</sub> plasma treatment were noted by Yildirim et al. [49]. The analysis of cell viability and adhesion in this paper demonstrates that the results are consistent with the literature data.

To better understand the cause of changes in the viability and adhesion of L929 cells on SXR/EUV and plasma O<sub>2</sub> or N<sub>2</sub> modified PCL nonwovens, it is worth considering the role of functional groups on the polymer surface because they influence cell behaviour [50]. Oxygen plasma treatment enters functional groups such as OH or COOH increasing hydrophilicity and promoting binding sites for integrin receptors on cells [30]. Abarrategi et al. [51] noted that the presence of variously charged functional groups (-CH<sub>3</sub>, -OH, -COOH, and -NH<sub>2</sub> groups) on the surface regulate the adsorption of fibronectin via binding integrins. The cell adhesion would be increased as follows: OH > COOH=NH<sub>2</sub> > CH<sub>3</sub>. Based on the XPS results (Table 1, 2) PCL surface treated with low-temperature oxygen plasma was enriched with a higher number of OH groups (Table 1) (O3, O5) and other oxygen-related groups (C3, C4, C6) compared to both control sample and PCL treated with nitrogen plasma. It indicates the presence of the stronger negatively charged surface of PCL treated with oxygen plasma compared to other samples and the surface charge is also a key factor affecting cell adhesion. It was shown that the negative charge on the surface can promote the adsorption of proteins enhancing cell adhesion [29,52], and strong adhesion to the substratum promote high cell proliferation [19,21]. Moreover, the presence of additional functional groups (Table 1) regulating surface charge and polarity can be responsible for increased viability and significant cell-surface adhesion of fibroblasts on PCL nonwoven treated with oxygen plasma.

Many reports investigate also the influence of uniformity of the

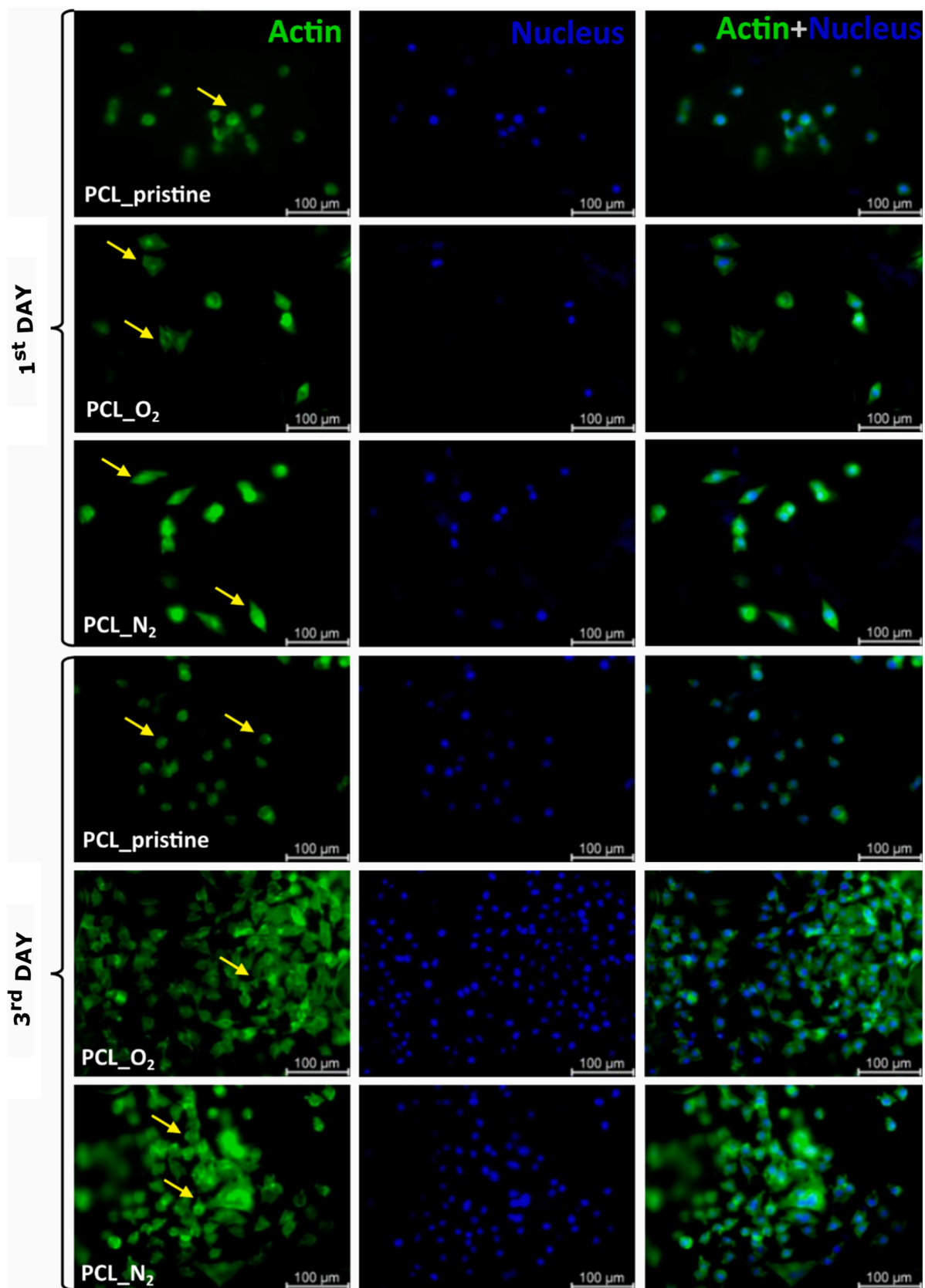


**Fig. 10.** L929 cells cultivated on: untreated PCL (PCL\_pristine), PCL treated with SXR/EUV radiation and low-temperature oxygen (PCL\_O<sub>2</sub>), and nitrogen (PCL\_N<sub>2</sub>) plasma for 1 and 3 days. Yellow arrows indicate differences in cell adhesion under the studied conditions. The F-actin (green, left column) and nuclei (blue, middle column) staining of L929 cells are visualized. The merge view is presented in the right column. The scale bar is 100 μm. (For interpretation of the references to colour in this figure legend, the reader is referred to the web version of this article.)

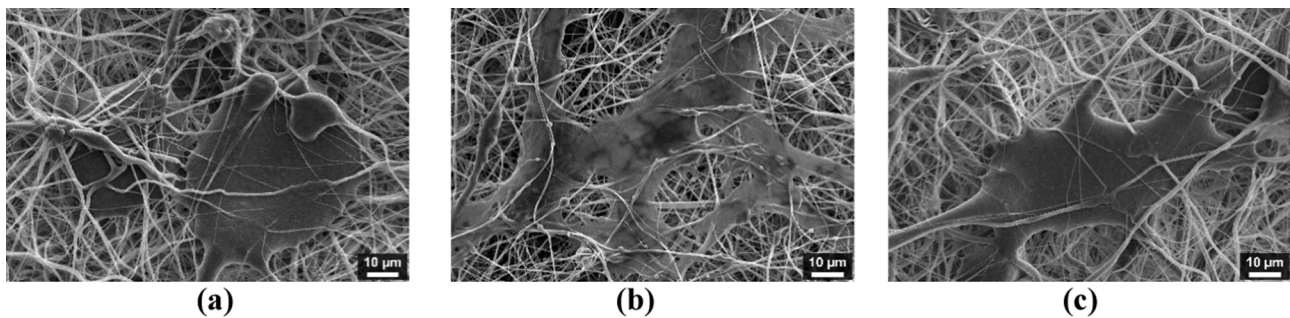


**Fig. 11.** SEM images of L929 fibroblast cells after 3 days of culture on: (a) pristine PCL, PCL treated with SXR/EUV radiation and low-temperature (b) oxygen, and (c) nitrogen plasma. Scale bars indicated.

scaffolds on cell attachment. It was shown that better uniformity of the scaffolds structure enhances cell adhesion [53,54]. According to the fiber diameter diagram (see Fig. 3), plasma-treated surfaces possess a much more even and uniform structure because the part of the fibers with the smallest diameter was removed after plasma treatment. Moreover, the most uniform diagram of the fiber diameter was observed on the oxygen plasma-treated sample. The effect is presented in Fig. 3a. Thus it also can confirm the better spreading and adhesion of cells on those surfaces. A similar plasma-treated effect was observed elsewhere [18].

To sum up, in this study increased viability of L929 was achieved on both oxygen and nitrogen-modified surfaces compared to the control. However, the effect of the sample treatment with oxygen plasma was much more significant compared to that of nitrogen plasma. Better cell adhesion on plasma-modified surfaces, in particular, with oxygen plasma, correlates with a higher proliferation of L929 fibroblasts.

#### 4. Conclusions

In this work, the influence of usage of a novel technique of modification, i.e. SXR/EUV radiation and two low-temperature, SXR/EUV induced, oxygen and nitrogen plasmas, on physico-chemical and biological properties of electrospun PCL nonwovens was presented. It was found that such modification did not significantly change the porous, three-dimensional structure of the fibrous PCL scaffolds. The PCL fibers were unbroken nor fused. It was observed that the thinnest fibers with diameters below  $\sim 400$  nm were ablated which led to more symmetric fiber diameter distributions with slightly higher average diameters. However, the interaction of SXR/EUV radiation and two types of low-temperature plasmas with the surfaces of the PCL nonwovens induced strong chemical alteration of their surfaces. It was observed that various new functional groups appeared on the surface of fibers, such as  $\text{CH}_3\text{-C}^*\text{-COO}$ ,  $\text{C-O-C}$ ,  $\text{C-N}$ ,  $\text{N-C=O}$  or  $\text{N-C-O}$ . The incorporation of 5.9 at.% nitrogen atoms (when modified with nitrogen plasma) and the increase in the percentage content of oxygen atoms of  $\sim 2.3$  at.% (when modified with oxygen plasma), compared to non-modified PCL mat, were noticed. The impact of these physico-chemical changes of modified PCL samples on the viability, morphology, and adhesion of L929 mouse fibroblasts was examined. All modified PCL surfaces were found not to be cytotoxic to cells. A significant increase in the viability of fibroblasts on both  $\text{O}_2$  and  $\text{N}_2$  plasma-treated PCL structures, compared to the non-modified sample, was observed. However, the effect was stronger for the samples treated with oxygen plasma than those treated with nitrogen plasma. Also, better adhesion on all modified PCL mats, compared to PCL pristine, was noticed – especially on PCL samples modified with oxygen plasma which resulted in a higher proliferation of L929 in this case. Therefore, based on the presented results, it can be concluded that the novel technique applied may be considered an interesting, useful, and attractive tool for surface bioactivation of various fibrous electrospun polymeric materials to be used in tissue engineering or biomedicine. However, further in-depth research on this

subject is required.

#### CRediT authorship contribution statement

**Joanna Czwartos:** Conceptualization, Investigation, Resources, Formal analysis, Methodology, Visualization, Writing – original draft, Funding acquisition. **Angelika Zaszczynska:** Investigation, Resources, Writing – review & editing. **Agata Nowak-Stępniewska:** Formal analysis, Visualization, Writing – review & editing. **Tomasz Fok:** Visualization, Writing – review & editing. **Bogusław Budner:** Formal analysis, Visualization. **Andrzej Bartnik:** Writing – review & editing. **Przemysław Wachulak:** Writing – review & editing. **Dorota Kołbuk:** Investigation, Writing – review & editing. **Paweł Sajkiewicz:** Writing – review & editing. **Henryk Fiedorowicz:** Writing – review & editing.

#### Declaration of Competing Interest

The authors declare that they have no known competing financial interests or personal relationships that could have appeared to influence the work reported in this paper.

#### Data availability

Data will be made available on request.

#### Funding

This research was supported by the National Science Centre, Poland, grant agreement no. UMO-2019/03/X/ST5/01643 and co-financed by Military University of Technology under research project UGB 731/2022.

#### References

- [1] P.X. Ma, Scaffolds for tissue fabrication, *Mater. Today* 7 (2004) 30–40, [https://doi.org/10.1016/S1369-7021\(04\)00233-0](https://doi.org/10.1016/S1369-7021(04)00233-0).
- [2] A. Zaszczynska, P. Sajkiewicz, A. Gradys, Piezoelectric scaffolds as smart materials for neural tissue engineering, *Polymers* 12 (2020) 1–19, <https://doi.org/10.3390/polym12010161>.
- [3] V. Guarino, M.G. Raucci, A. Ronca, V. Cirillo, L. Ambrosio, Multifunctional scaffolds for bone regeneration, *Bone Substit. Biomater.* 5 (2014) 95–117, <https://doi.org/10.1533/9780857099037.2.95>.
- [4] S. Yang, K.F. Leong, Z. Du, C.K. Chua, The design of scaffolds for use in tissue engineering. Part 1. Traditional factors, *Tissue Eng.* 7 (2001) 679–689, <https://doi.org/10.1089/107632701753337645>.
- [5] D.W. Hutmacher, Scaffold design and fabrication technologies for engineering tissues—state of the art and future perspectives, *J. Biomater. Sci.-Polym. Ed.* 12 (2001) 107–124, <https://doi.org/10.1163/156856201744489>.
- [6] J. Litowczenko, M.J. Wozniak-Budych, K. Staszak, K. Wieszczycka, S. Jurga, B. Tylkowski, Milestones and current achievements in development of multifunctional bioscaffolds for medical application, *Bioact. Mater.* 6 (2021) 2412–2438, <https://doi.org/10.1016/j.bioactmat.2021.01.007>.
- [7] E.V. Melnik, S.N. Shkarina, S.I. Ivlev, V. Weinhardt, T. Baumbach, M.V. Chaikina, M.A. Surmeneva, R.A. Surmenev, In vitro degradation behaviour of hybrid electrospun scaffolds of polycaprolactone and strontium-containing hydroxyapatite

- microparticles, *Polym. Deg. Stab.* 167 (2019) 21–32, <https://doi.org/10.1016/j.polydegradstab.2019.06.017>.
- [8] F.H. Zulkifli, F.S. Hussain, M.S. Rasad, M.M. Yusoff, In vitro degradation study of novel HEC/PVA/collagen nanofibrous scaffold for skin tissue engineering applications, *Polym. Deg. Stab.* 110 (2014) 473–481, <https://doi.org/10.1016/j.polydegradstab.2014.10.017>.
- [9] H.W. Choi, J. Johnson, D.F. Farson, J. Lannutti, Femtosecond laser structuring of PCL and PET electrospun nanofiber mesh, *ICALEO M 203* (2006) 135–142, <https://doi.org/10.2351/1.5060882>.
- [10] Z. Ma, W. He, S. Yong, S. Ramakrishna, Grafting of gelatin on electrospun poly (caprolactone) nanofibers to improve endothelial cell spreading and proliferation and to control cell orientation, *Tissue Eng.* 11 (2005) 1149–1158, <https://doi.org/10.1089/ten.2005.11.1149>.
- [11] A. Yazdanpanah, Z. Madjid, M. Pezeshki-Modares, Z. Khosrowpour, P. Farshi, L. Eini, J. Kiani, M. Seifi, S.C. Kundu, R. Ghods, M. Gholipourmalekabadi, Bioengineering of fibroblast-conditioned polycaprolactone gelatin electrospun scaffold for skin tissue engineering, *Artif. Organs* 46 (2022) 1040–1054, <https://doi.org/10.1111/aor.14169>.
- [12] S. Sharif, J. Ai, M. Azami, J. Verdi, M.A. Atlasi, S. Shirian, A. Samadikuchaksaraei, Collagen-coated nano-electrospun PCL seeded with human endometrial stem cells for skin tissue engineering applications, *J. Biomed. Mater. Res. B Appl. Biomater.* 106 (2018) 1578–1586, <https://doi.org/10.1002/jbm.b.33966>.
- [13] Z. Cheng, S.-H. Teoh, Surface modification of ultra thin poly ( $\epsilon$ -caprolactone) films using acrylic acid and collagen, *Biomaterials* 25 (2004) 1991–2001, <https://doi.org/10.1016/j.biomaterials.2003.08.038>.
- [14] K.D. Patel, T.-H. Kim, N. Mandakhbayar, R.K. Singh, J.-H. Jang, J.-H. Lee, H.-W. Kim, Coating biopolymer nanofibers with carbon nanotubes accelerates tissue healing and bone regeneration through orchestrated cell- and tissue-regulatory responses, *Acta Biomater.* 108 (2020) 97–110, <https://doi.org/10.1016/j.actbio.2020.03.012>.
- [15] N. Fazeli, E. Arefian, S. Irani, A. Ardeshtyrlajimi, E. Seyedjafari, 3D-printed PCL scaffolds coated with nanobioceramics enhance osteogenic differentiation of stem cells, *ACS Omega* 6 (2021) 35284–35296, <https://doi.org/10.1021/acsomega.1c04015>.
- [16] F. Chen, C.N. Lee, S.H. Teoh, Nanofibrous modification on ultra-thin poly ( $\epsilon$ -caprolactone) membrane via electrospinning, *Mater. Sci. Eng. C* 27 (2007) 325–332, <https://doi.org/10.1016/j.msec.2006.05.004>.
- [17] O. Jeznach, D. Kolbuk, M. Marzec, A. Bernasik, P. Sajkiewicz, Aminolysis as a surface functionalization method of aliphatic polyester nonwovens: impact on material properties and biological response, *RSC Adv.* 12 (2022) 11303–11317, <https://doi.org/10.1039/d2ra00542e>.
- [18] A.M. Pappa, V. Karagkiozaki, S. Krol, S. Kassavetis, D. Konstantinou, C.h. Pitsalidis, L. Tzounis, N. Pliatsikas, S. Logothetidis, Oxygen-plasma-modified biomimetic nanofibrous scaffolds for enhanced compatibility of cardiovascular implants, *Beilstein J. Nanotechnol.* 6 (2015) 254–262, <https://doi.org/10.3762/bjnano.6.24>.
- [19] S. Siro, P. Wadubua, V. Amornkitbamrung, N. Kampa, S. Maensiri, Surface modification of electrospun PCL scaffolds by plasma treatment and addition of adhesive protein to promote fibroblast cell adhesion, *Mater. Sci. Technol.* 26 (2010) 1292–1297, <https://doi.org/10.1179/026708310X12798718274070>.
- [20] M. Sivan, D. Madheswaran, M. Asadian, P. Cools, M. Thukkaram, P. Voort, R. Morent, N. Geyter, D. Lukas, Plasma treatment effects on bulk properties of polycaprolactone nanofibrous mats fabricated by uncommon AC electrospinning: a comparative study, *Surf. Coat. Technol.* 399 (2020) 1–11, <https://doi.org/10.1016/j.surfcoat.2020.126203>.
- [21] M. Asadian, M. Dhaenens, I. Onyshchenko, S. Wael, H. Declercq, P. Cools, B. Devreese, D. Deforce, R. Morent, N. Geyter, Plasma functionalization of polycaprolactone nanofibers changes protein interactions with cells, resulting in increased cell viability, *ACS Appl. Mater. Interfaces* 10 (2018) 41962–41977, <https://doi.org/10.1021/acami.8b14995>.
- [22] P. Slepicka, N. Slepickova Kasalkova, E. Stranska, L. Bacakova, V. Svorcik, Surface characterization of plasma treated polymers for applications as biocompatible carriers, *EXPRESS Polym Lett.* 7 (2013) 535–545, <https://doi.org/10.3144/expresspolymlett.2013.50>.
- [23] K. Nezelova, D. Fajstavr, S. Rimpelova, N. Slepickova Kasalkova, Z. Kolska, V. Svorcik, P. Slepicka, Honeycomb-patterned poly(L-lactic) acid on plasma-activated FEP as cell culture scaffold, *Polym. Deg. Stab.* 181 (2020) 109370, <https://doi.org/10.1016/j.polydegradstab.2020.109370>.
- [24] P. Slepicka, N. Slepickova Kasalkova, J. Siegel, Z. Kolska, L. Bacakova, V. Svorcik, Nano-structured and functionalized surfaces for cytocompatibility improvement and bactericidal action, *Biotechnol. Adv.* 33 (2015) 1120–1129, <https://doi.org/10.1016/j.biotechadv.2015.01.001>.
- [25] N. Slepickova Kasalkova, P. Slepicka, L. Bacakova, P. Sajdl, V. Svorcik, Biocompatibility of plasma nanostructured biopolymers, *Nucl. Instrum. Methods Phys. Res. B* 307 (2013) 642–646, <https://doi.org/10.1016/j.nimb.2012.10.035>.
- [26] P. Slepicka, N. Slepickova Kasalkova, A. Pinker, P. Sajdl, Z. Kolska, V. Svorcik, Plasma induced cytocompatibility of stabilized poly-L-lactic acid doped with graphene nanoplatelets, *React. Funct. Polym.* 131 (2018) 266–275, <https://doi.org/10.1016/j.reactfunctpolym.2018.08.006>.
- [27] A. Martins, D.E. Pinho, S. Faria, I. Pashkuleva, A.P. Marques, L.R. Reis, N.M. Neves, Surface modification of electrospun polycaprolactone nanofiber meshes by plasma treatment to enhance biological performance, *Small* 5 (2009) 1195–1206, <https://doi.org/10.1002/sml.200801648>.
- [28] A.A. Ivanova, D.S. Syromotina, S.N. Shkarina, R. Shkarin, A. Cecilia, V. Weinhardt, T. Baumbach, M.S. Saveleva, D.A. Gorin, T.E.L. Douglas, B.V. Parakhonkiy, A. G. Skirtach, P. Cools, N. Geyter, R. Morent, C. Oehr, M.A. Surmeneva, R. A. Surmenev, Effect of low-temperature plasma treatment of electrospun polycaprolactone fibrous scaffolds on calcium carbonate mineralization, *RSC Adv.* 8 (2018) 39106–39114, <https://doi.org/10.1039/C8RA07386D>.
- [29] E. Stastna, K. Castkova, J. Rahel, Influence of hydroxyapatite nanoparticles and surface plasma treatment on bioactivity of polycaprolactone nanofibers, *Polymers* 12 (2020) 1–16, <https://doi.org/10.3390/polym12091877>.
- [30] F. Ghorbani, M. Sahanavard, A. Zamanian, Immobilization of gelatin on the oxygen plasma-modified surface of polycaprolactone scaffolds with tunable pore structure for skin tissue engineering, *J. Polym. Res.* 27 (2020) 1–12, <https://doi.org/10.1007/s10965-020-02263-6>.
- [31] A. Bartnik, W. Lisowski, J. Sobczak, P. Wachulak, B. Budner, B. Korczyk, H. Fiedorowicz, J. Kostecki, EUV induced ablation and surface modification of poly (vinylidene fluoride) irradiated in vacuum or gaseous environment, *877708-1*, *Proc. SPIE* 8777 (2013), <https://doi.org/10.1117/12.2021152>.
- [32] A. Bartnik, H. Fiedorowicz, R. Jarocki, J. Kostecki, A. Szczurek, M. Szczurek, P. Wachulak, EUV-induced nanostructuring of solids, *Acta Phys. Pol. A* 121 (2012) 445–449, <https://doi.org/10.12693/APhysPolA.121.445>.
- [33] A. Bartnik, H. Fiedorowicz, R. Jarocki, J. Kostecki, A. Szczurek, M. Szczurek, Ablation and surface modifications of PMMA using a laser-plasma EUV source, *Appl. Phys. B* 96 (2009) 727–730, <https://doi.org/10.1007/s00340-009-3692-8>.
- [34] A. Bartnik, H. Fiedorowicz, R. Jarocki, J. Kostecki, M. Szczurek, A. Szczurek, P. Wachulak, EUV-induced ablation and surface modifications of solids, *80770H-1*, *Proc. SPIE* 8077 (2011), <https://doi.org/10.1117/12.887491>.
- [35] A. Bartnik, W. Lisowski, J. Sobczak, P. Wachulak, B. Budner, B. Korczyk, H. Fiedorowicz, Simultaneous treatment of polymer surface by EUV radiation and ionized nitrogen, *App. Phys. A* 109 (2012) 39–43, <https://doi.org/10.1007/s00339-012-7243-5>.
- [36] J. Czwartos, B. Budner, A. Bartnik, P. Wachulak, H. Fiedorowicz, Z. Mierczyk, Physico-chemical surface modifications of polyetheretherketone (PEEK) using extreme ultraviolet (EUV) radiation and EUV induced nitrogen plasma, *Materials* 13 (2020) 4466, <https://doi.org/10.3390/ma13194466>.
- [37] J. Czwartos, B. Budner, A. Bartnik, W. Kasprzycka, H. Fiedorowicz, Effect of photoionized plasma and EUV induced surface modification on physico-chemical properties and cytocompatibility of PLLA, *EXPRESS Polym. Lett.* 14 (2020) 1063–1077, <https://doi.org/10.3144/expresspolymlett.2020.86>.
- [38] J. Czwartos, B. Budner, A. Bartnik, P. Wachulak, B.A. Butruk-Raszeja, A. Lech, T. Ciach, H. Fiedorowicz, Effect of extreme ultraviolet (EUV) radiation and EUV induced, N<sub>2</sub> and O<sub>2</sub> based plasmas on a PEEK surface's physico-chemical properties and MG63 cell adhesion, *Int. J. Mol. Sci.* 22 (2021) 8455, <https://doi.org/10.3390/ijms22168455>.
- [39] P. Denis, J. Dulnik, P. Sajkiewicz, Electrospinning and structure of biocomponent polycaprolactone/gelatin nanofibers obtained using alternative solvent system, *Int. J. Polym. Mater. Polym. Biomater.* 64 (2015) 354–364, <https://doi.org/10.1080/00914037.2014.945208>.
- [40] H. Fiedorowicz, A. Bartnik, R. Jarocki, J. Kostecki, J. Krzywiński, J. Mikolajczyk, R. Rakowski, A. Szczurek, M. Szczurek, Compact laser plasma EUV source based on a gas puff target for metrology applications, *J. Alloys Compd.* 401 (2005) 99–103, <https://doi.org/10.1016/j.jallcom.2005.02.069>.
- [41] P.W. Wachulak, Contributed Review: The novel gas puff targets for laser-matter interaction experiments, *Rev. Sci. Instrum.* 87 (9) (2016) 091501, <https://doi.org/10.1063/1.4962012>.
- [42] D. Kolbuk, S. Guimond-Lischer, P. Sajkiewicz, K. Maniura-Weber, G. Fortunato, The effect of selected electrospinning parameters on molecular structure of polycaprolactone nanofibers, *Int. J. Polym. Mater. Polym. Biomater.* 64 (2015) 365–377, <https://doi.org/10.1080/00914037.2014.945209>.
- [43] G.E. Simmonds, J.D. Bomberger, M.A. Bryner, Designing nonwovens to meet pore size specifications, *J. Eng. Fibers Fabrics* 2 (1) (2007) 1–15, <https://doi.org/10.1177/155892500700200101>.
- [44] Y. Wan, C. Tu, J. Yang, J. Bei, S. Wang, Influences of ammonia plasma treatment on modifying depth and degradation of poly(L-lactide) scaffolds, *Biomaterials* 27 (2006) 2699–2704, <https://doi.org/10.1016/j.biomaterials.2005.12.007>.
- [45] M. Asadian, I. Onyshchenko, D. Thiry, P. Cools, H. Declercq, R. Snyders, R. Morent, N. Geyter, Thiolation of polycaprolactone (PCL) nanofibers by inductively coupled plasma (ICP) polymerization: physical, chemical and biological properties, *Appl. Surf. Sci.* 479 (2019) 942–952, <https://doi.org/10.1016/j.apsusc.2019.02.178>.
- [46] I. Ul Ahad, B. Butruk, M. Ayele, B. Budner, A. Bartnik, H. Fiedorowicz, T. Ciach, D. Brabazon, Extreme ultraviolet (EUV) surface modification of polytetrafluoroethylene (PTFE) for control of biocompatibility, *Nucl. Instrum. Methods Phys. Res. B* 364 (2015) 98–107, <https://doi.org/10.1016/j.nimb.2015.08.093>.
- [47] S. Cai, C. Wu, W. Yang, W. Liang, H. Yu, H. Liu, Recent advance in surface modification for regulating cell adhesion and behaviors, *Nanotechnol. Rev.* 9 (2020) 971–989, <https://doi.org/10.1515/ntrev-2020-0076>.
- [48] N. Recek, M. Resnik, H. Motaln, T. Lah-Turnšek, R. Augustine, N. Kalarikkal, S. Thomas, M. Mozetič, Cell adhesion on polycaprolactone modified by plasma treatment, *Int. J. Polym. Sci.* 2016 (2016) 1–9, <https://doi.org/10.1155/2016/7354396>.
- [49] E.D. Yildirim, D. Pappas, S. Guceri, W. Sun, Enhanced cellular functions on polycaprolactone tissue scaffolds by O<sub>2</sub> plasma surface modification, *Plasma Process. Polym.* 8 (2011) 256–267, <https://doi.org/10.1002/ppap.201000009>.
- [50] J.H. Lee, H.W. Jung, I.K. Kang, H.B. Lee, Cell behaviour on polymer surfaces with different functional groups, *Biomaterials* 15 (1994) 705–711, [https://doi.org/10.1016/0142-9612\(94\)90169-4](https://doi.org/10.1016/0142-9612(94)90169-4).
- [51] A. Abarrategi, Y. López-Morales, V. Ramos, A. Civantos, L. López-Durán, F. Marco, J.L. Lopez-Lacomba, Chitosan scaffolds for osteochondral tissue regeneration, *J. Biomed. Mater. Res. Part A* 95 (2010) 1132–1141, <https://doi.org/10.1002/jbm.a.32912>.

- [52] P. Thevenot, W. Hu, L. Tang, Surface chemistry influences implant biocompatibility, *Curr. Top. Med. Chem.* 8 (2008) 270–280, <https://doi.org/10.2174/156802608783790901>.
- [53] M. Chen, P.K. Patra, S. Bhowmick, Role of fiber diameter in adhesion and proliferation of NIH 3T3 fibroblasts on electrospun polycaprolactone scaffolds, *Tissue Eng.* 13 (2007) 579–587, <https://doi.org/10.1089/ten.2006.0205>.
- [54] M. Chen, P.K. Patra, M.L. Lovett, D.L. Kaplan, S. Bhowmick, Role of electrospun fibre diameter and corresponding specific surface area (SSA) on cell attachment, *J. Tissue Eng. Regen. Med.* 3 (2009) 269–279, <https://doi.org/10.1002/term.163>.